Fermi National Accelerator Laboratory

FERMILAB-Pub-79/51-EXP
7420.180
(Submitted to Nucl. Phys. B.)

PROPERTIES OF K^0 and Λ INCLUSIVE PRODUCTION IN CHARGED-CURRENT ANTINEUTRINO-NUCLEON INTERACTIONS

V. Ammosov, A. Amrakhov, A. Denisov, P. Ermolov,
V. Gapienko, V. Klyukhin, V. Koreshev, P. Pitukhin,
V. Sirotenko, E. Slobodyuk and V. Zaetz
Institute of High Energy Physics, Serpukhov, USSR

and

J. P. Berge, D. Bogert, R. Endorf, R. Hanft, J. Malko,
G. Moffatt, F. Nezrick and J. Wolfson
Fermi National Accelerator Laboratory
Batavia, Illinois 60510, USA

and

V. Efremenko, A. Fedotov, P. Gorichev, F. Kaftanov,
G. Kliger, V. Kolganov, S. Krutchinin, M. Kubantsev,
I. Makhlyueva, V. Shekeljan and V. Shevchenko
Institute of Theoretical and Experimental Physics, Moscow, USSR

July 1979

PROPERTIES OF K^0 and Λ INCLUSIVE PRODUCTION IN CHARGED-CURRENT ANTINEUTRINO-NUCLEON INTERACTIONS

V. Ammosov, A. Amrakhov, A. Denisov, P. Ermolov,
V. Gapienko, V. Klyukhin, V. Koreshev, P. Pitukhin,
V. Sirotenko, E. Slobodyuk and V. Zaetz
Institute of High Energy Physics, Serpukhov, USSR

and

J. P. Berge, D. Bogert, R. Endorf,* R. Hanft, J. Malko,
G. Moffatt,* F. Nezrick and J. Wolfson
Fermi National Accelerator Laboratory
Batavia, Illinois 60510, USA

and

V. Efremenko, A. Fedotov, P. Gorichev, F. Kaftanov,
G. Kliger, V. Kolganov, S. Krutchinin, M. Kubantsev,
I. Makhlyueva, V. Shekeljan and V. Shevchenko
Institute of Theoretical and Experimental Physics, Moscow, USSR

*Visitor from University of Cincinnati

ABSTRACT

In this paper we discuss inclusive spectra of K^{o}'s and Λ's produced in charged-current $\bar{\nu}_{\mu}N$ interactions in the Fermilab 15-ft bubble chamber filled with a 64% Ne-H_2 mixture. Data presented in terms of the invariant cross section show, when compared with results from experiments with other incident beams, that the behavior of these distributions is approximately the same. The K^{o} and Λ fragmentation functions are presented and the shape of the K^{o} fragmentation function is found to be consistent with the parameterization of Field and Feynman.

The average K^{o} and Λ transverse momentum squared as a function of Q^2, W^2, x and z is presented. Comparisons for the K^{o}'s produced in the current fragmentation region are in qualitative agreement with QCD predictions. The value of the Λ polarization is measured and a positive normal polarization $P_N = 0.34 \pm 0.18$ is found.

I. INTRODUCTION

Deep-inelastic antineutrino-nucleon scattering is commonly interpreted as the scattering of a virtual intermediate boson W^- of mass Q^2 and energy ν from the quarks contained in the nucleon. Within this context, the W^- strikes a quark in the nucleon and changes it to a quark with different flavor, which then fragments into the observed hadrons. This approach has been successful in analyzing the pion production in antineutrino, neutrino, electroproduction and e^+e^- data.[1] Measurements of the antineutrino production of K^o's can add considerably to our knowledge of the hadron production mechanism in deep-inelastic processes. A study of Λ's produced in antineutrino-nucleon interaction allows one to understand the systematic trends for the target fragments, i.e., hadrons from the remaining two-quark system. There are as yet little data concerning K^o and Λ inclusive production by neutrinos and antineutrinos.[2,3] Most of the information on strange particle production with lepton beams comes from ep and e^+e^- experiments.[4-7]

We have collected a sample of charged-current $\bar{\nu}N$ events having a visible neutral strange particle decay in the final state, $\bar{\nu}N \to \mu^+ V^o X$, where V^o stands for $K^o_s \to \pi^+\pi^-$ or $\Lambda \to p\pi^-$, and X is the rest of the hadronic system. The general features of the production mechanism of this data sample have been studied in terms of variables used in weak and strong interaction physics. Production rates, a search for charmed particle effects in invariant mass distributions and an indirect study of charm effects via V^o's in

charged-current interactions will be published in a separate forthcoming paper.

In Section II we discuss the event selection. Section III deals with inclusive neutral strange particle distributions. In Section IV we present the average transverse momentum behavior as a function of Q^2, W^2, x and z and the corresponding QCD predictions. In Section V we discuss the Λ polarization effects. The major conclusions are summarized in Section VI.

II. EVENT SELECTION

The data come from the exposure of the Fermilab 15-ft bubble chamber filled with a heavy neon-hydrogen mixture (64 atm percent of neon, density 0.73 g/cm^3) to a high energy antineutrino beam. This exposure of 85,000 pictures was made with a wide-band double-horn focused beam with $9.15 \cdot 10^{17}$ protons at 400 GeV on target. The peak in the antineutrino flux distribution is at $\sim$12 GeV, but the spectrum extends to above 100 GeV.

The film was scanned for all neutral-induced interactions with one or more charged prongs which then were measured and processed through a geometrical reconstruction program. To study the inclusive V^0 (Λ and K^0_s) production we processed through a kinematic program[8] the measurements of those events having one or more possible associated two-prong decays. For all fits we have employed a confidence-level cut of 0.001. We considered a V^0 to be a γ-ray conversion if it had both leaving tracks without visible

kinks or secondary interactions and a constrained γ fit for which the positron momentum transverse to the V^o direction was less than 40 MeV/c. This procedure resulted in losses of K_s^o and Λ equal to $\sim$1% and a γ contamination in the neutral strange particle sample of $\sim$0.5%. The ambiguities between Λ and K_s^o ($\sim$18%) were statistically separated using the difference between the transverse momentum distribution of the negative decay track from the Λ and K_s^o respectively. To resolve the ambiguities the following expression was used:

$$W_A/W_B = f_A(P_t)N_A\, e^{-\chi_A^2/2} / (f_B(P_T)N_B\, e^{-\chi_B^2/2}); \quad \sum_i W_i = 1$$

where W_i is the weight for i-th hypothesis with fit χ_i^2, N_i is the number of unambiguous particles of kind i, and $f_i(P_T)$ is the distribution function of negative particle transverse momentum with respect to the V^o direction assuming an isotropic decay in the V^o rest frame. In addition, we ignored any Λ or K_s^o fit having a proper time greater than five lifetimes, a projection length from the primary vertex to V^o vertex less than 0.8 cm or a distance from the V^o vertex to the chamber wall along the direction of V^o line of flight less than 20 cm. To compensate for V^o's which are removed by these potential-length cuts weights were calculated in the conventional way. After this all Λ's and K_s^o's were weighted for neutral decay modes (including K_L^o), scanning and processing inefficiencies. In the following by K^o we mean both K^o and $\overline{K^o}$.

A check on the method used to resolve ambigities is shown in figures 1 and 2. Figure 1 gives the distributions of events with

respect to θ, the angle between one of the V^o decay products and the incoming V^o direction in the V^o rest frame. These angular distributions are consistent with being isotropic. The distributions of $c\tau$ are shown in Fig. 2 for K_s^o and Λ decays. For each distribution in Fig. 2 we have made a maximum likelihood fit to the theoretical form and obtained values of $c\tau$ equal to 2.85 ± 0.16 and 7.26 ± 0.44 cm for K_s^o and Λ, respectively, which are in good agreement with the known lifetimes.

In Fig. 3 we present the effective mass distributions for the K^o and Λ samples. As can be seen from this figure, assigning the correct masses to the decay particles results in invariant mass squared distributions for the K^o and Λ that have the average values of 0.248 and 1.247 GeV^2/c^4 with widths of 0.032 and 0.017 GeV^2/c^4, respectively, indicating good experimental resolution.

The charged-current events were obtained by requiring that the primary events were inside a fiducial volume of $\sim$17 m^3, that there was a selected positive muon and that the reconstructed energy of each event, $E_{\bar{\nu}}$, was greater than 10 GeV. Muons were identified by the External Muon Identifier (EMI)[9] and/or a kinematic method[10] and were required to have momentum greater than 4 GeV/c. The anti-neutrino energy was estimated[11] using an average correction for neutral energy loss characteristic of the total event sample from this run. The energy resolution is equal to $\sim$10% but results presented in this paper are not significantly sensitive to the particular energy - estimation method employed. In Table I we give the observed and corrected number of events for the different V^o topologies.

III. INCLUSIVE MOMENTUM SPECTRA

To study the inclusive neutral strange particle production we have employed variables normally used in hadron induced reactions. These variables are x_F, the Feynman scaling variable, defined here as $x_F = 2\,P_L^*/\sqrt{s}$, and P_T^2, the squared transverse - momentum of a particle with respect to the incident beam direction. Here P_L^* is the component of particle momentum along the beam direction in the center of mass system (c.m.s.), and $\sqrt{s}$ is the center of mass energy. In antineutrino - induced reactions the corresponding c.m.s. frame is the hadronic rest system with the beam direction defined as being opposite to the target nucleon direction in this system and $\sqrt{s} = W$, the total hadronic effective mass. These two variables depend on the measured K^o and Λ momenta and can be sensitive to differences between production mechanisms.

The transverse momentum distributions for the K^o and the Λ are shown in Fig. 4. These distributions give good fits to $dN/dP_T^2 \sim \exp(-B\,P_T^2)$ forms with slopes 4.31 ± 0.35 ($\chi^2/ND = 5.2/7$) and 4.45 ± 0.32 ($\chi^2/ND = 1.7/6$) for K^o and Λ. This K^o slope is similar to that obtained from $\pi^- p$ data[12] (4.59 ± 0.11), and less then that obtained from νp data[3] (7.1 ± 1.4). Our slope for the Λ distribution is consistent with that found for Λ production from charged-current νp interactions (5.8 ± 1.1) but greater than obtained from the $\pi^- p$ experiment (3.62 ± 0.13).

To investigate the production dynamics in more detail we define the invariant cross section for K^o and Λ as

$$\phi(x_F, P_T^2) = (1/N_T)(E^*/W)\ d^2n/dx_F dP_T^2$$

Here E^* is the V^O energy in the hadron rest frame, W is the total hadron effective mass, N_T is the total number of inelastic charged-current events and n is the number of K^O's or Λ's. We note that for V^O charged-current events the average value of W^2 is equal to $\sim$20 GeV^2 and the average value of Q^2 (square of the four-momentum transfer between the incident antineutrino and outgoing muon) equals $\sim$5 GeV^2/c^2.

In Fig. 5 we present the K^O and Λ invariant x_F distributions $F(x_F) = \int\phi(x_F, P_T^2)dP_T^2$. For comparison we show the data obtained from νp, $\pi^- p$ and ep experiments[3,12,4] normalized to our data in the corresponding overlapping x_F regions. One can see that within errors all distributions show the same qualitative behavior. As expected most Λ's are produced in the target fragmentation region while the $F(x_F)$ distribution for the K^O sample is shifted towards the current fragmentation region.

The invariant P_T^2 distributions $G(P_T^2) = \int\phi(X_F, P_T^2)dX_F$ for K^O and Λ are given in Fig. 6. These distributions are exponential in P_T^2 with slope parameters of 3.80 ± 0.47 ($\chi^2/ND = 4.7/7$) and 4.36 ± 0.51 ($\chi^2/ND = 4.9/6$) for the K^O and Λ, respectively. The value of the K^O slope is in good agreement with the measured slope for K^O's produced from $\pi^- p$ data[12] (3.91 ± 0.11). The Λ slope is consistent with the values for electroproduced Λ's and protons[13] but greater than that obtained from the $\pi^- p$ data (3.24 ± 0.13).

In Fig. 7a we show the K^O z distribution dn/dz, for our data. Here z is the Lorentz invariant quantity hp/pQ (h and p are the four-momenta of hadron and target) which in the laboratory system becomes $E_H/(E_{\bar{\nu}}-E_{\mu^+})$ where E_H is the particle energy in the laboratory. The solid line gives the result obtained using the parametrizations of the quark densities and fragmentation functions of Field and Feynman (FF2)[14] for the high z-region (z > 0.25). The data are in qualitative agreement with the FF2 prediction. For comparison we also show the data for K^O production in ep interactions[6] and νN interactions,[15] normalized to our data in the high z region.

The z distribution for Λ is presented in Fig. 7b. A possible plateau in the Λ spectrum at high z may be connected with quasi-elastic production of Λ hyperons. The solid curve shows the behavior dn/dz for electroproduced protons[16] and the open triangles give the Λ data obtained from a νN experiment.[15] All these distributions have been normalized in the high z region. We note that all these distributions have a similar shape.

IV. AVERAGE TRANSVERSE MOMENTUM BEHAVIOR

One of the more interesting details of hadron production by neutrinos is the behavior of the average transverse momentum $< P_T >$ as a function of the variables Q^2, W^2, $x = Q^2/2m\nu$ and z. Some features of the $< P_T^2 >$ behavior can be predicted by quantum chromodynamics (QCD).[17] For example, $< P_T^2 >$ is expected to

increase with Q^2 as $Q^2/\ln(Q^2/\Lambda^2)$ and to decrease with x at small x. However the study of $< P_T^2 >$ is complicated by the poor knowledge of the total hadron direction due to undetected neutrals.[18] Therefore we use instead the K^o and Λ momentum squared perpendicular to the well determined $\bar{\nu}\mu$ plane (P^2_{out}). The reason for choosing this variable is that the quantity $< P^2_{out} >$ has a maximum uncertainty $\sim 0.02\,GeV^2/c^2$ at our Q^2 range due to the antineutrino beam spread, the error on the muon momentum and the nucleon fermi motion. Also the $< P^2_{out} >$ variable should be more sensitive than $< P_{out} >$ since it will be influenced more by the high P^2_{out} tail.

In Fig. 8 we plot $< P^2_{out} >$ as a function of Q^2 for the K^o and Λ samples. One can see that no significant dependence $< P^2_{out} >$ on Q^2 is observed for the Λ data while the K^o data show some indication of slowly increasing $< P^2_{out} >$ with increasing Q^2. This rise becomes more marked if K^o mesons in the current fragmentation region ($z > 0.2$) are selected (black points).

To compare the QCD predictions for K^o production with our experimental data at the quantitative level we have calculated these predictions for our conditions following the methods of Ref. 19. The QCD calculation is obtained assuming azimuthal symmetry. To include the effects of primordial quark transverse momentum and the transverse momentum due to the quark fragmentation we add a constant Q^2 independent term to the QCD prediction, using the experimental value $< P^2_{out} > = 0.138 \pm .006$ obtained for $z > 0.2$. The results of the above theoretical calculation is shown by the solid curve in Fig. 8. We see that the $< P^2_{out} >$ dependence for

K^o's in the current fragmentation region is in qualitative agreement with the QCD prediction.

The $< P^2_{out} >$ behavior as a function of x is shown in Fig. 9 for the K^o's and Λ's. From Fig. 9 we see that $< P^2_{out} >$ for Λ is independent of x at least in the region $x > 0.1$. For K^o mesons $< P^2_{out} >$ decreases with increasing x. The solid curve in Fig. 9a shows the QCD predictions for the K^o's produced with $z > 0.2$. The K^o data are in good agreement with the theoretical predictions.

In Fig. 10 we present the W^2 dependence of $< P^2_{out} >$ for K^o and Λ. The curve again shows the corresponding QCD predictions for K^o mesons produced in the current fragmentation region ($z > 0.2$). We see that the K^o data are compatible with the QCD predictions. A comparison of figures 8a and 10a shows that for the K^o data $< P^2_{out} >$ increases more rapidly with increasing W^2 than increasing Q^2. This stronger dependence on W^2 is connected with the relation $W^2 \sim Q^2(1/x - 1)$, since high W^2 values correspond to both high Q^2 and small x. No evidence is seen for a W^2 dependence of $< P^2_{out} >$ in the Λ data, but the errors are rather large.

The $< P^2_{out} >$ behavior as a function of z is shown in figures 11a and b for the K^o's and Λ respectively. The K^o data exhibit the so called "seagull effect", where $< P^2_{out} >$ is seen to increase with increasing z. Again we see that the $< P^2_{out} >$ behavior for K^o meson does not contradict the QCD predictions (solid line). We note also that the Λ data appear to show a rise in $< P^2_{out} >$, although the errors are quite large.

V. INCLUSIVE Λ POLARIZATION

We have attempted to gain an estimate of the Λ polarization effects in our charged-current sample. We introduce an orthogonal system of coordinates

$$\hat{e}_x = \hat{e}_\Lambda; \quad \hat{e}_z = \frac{\hat{e}_\Lambda \times \hat{e}_{\bar{\nu}}}{|\hat{e}_\Lambda \times \hat{e}_{\bar{\nu}}|}; \quad \hat{e}_y = \hat{e}_z \times \hat{e}_x$$

where $\hat{e}_\Lambda$ ($\hat{e}_{\bar{\nu}}$) is the unit vector along the direction of motion of the Λ (antineutrino). The components of the Λ polarization along e_x, e_y and e_z are referred to as the longitudinal P_L, perpendicular P_T and normal P_N polarization, respectively. For events with Λ the angles θ_i of the decay proton (in the Λ-rest frame) with respect to the polarization directions have been calculated. For each cos θ_i distribution we have made a maximum likelihood fit to the theoretical distribution function

$$f(P, \cos\theta) = \frac{1}{2}(1 + \alpha P \cos\theta)$$

where α is the asymmetry parameter for Λ decay and its value is set equal to 0.647 ± 0.013.[20] The estimates of Λ polarization from these fits are

$$P_L = -0.15 \pm 0.20$$

$$P_T = -0.12 \pm 0.19$$

$$P_N = 0.34 \pm 0.18$$

The spin of the Λ will be the spin of the s-quark in a constituent quark approximation, since the (ud) pair is an isosinglet and spin singlet state. If $s\bar{s}$ pairs are produced by gluons we may expect a large normal polarization[21] of Λ hyperons in the appropriate x region.

The obtained values of longitudinal and perpendicular polarization (P_L and P_T) are compatible with zero within errors but a small positive P_N polarization effect does exist at the $\sim 2\sigma$ level. This P_N polarization is concentrated at small x, as can be seen in Fig. 12a which gives the polarization as a function of $x = Q^2/2m\nu$. In Fig. 13 we show the values of the Λ polarizations as a function of Q^2; no significant dependence on Q^2 is seen.

VI. SUMMARY

We have examined the details of the inclusive K^o and Λ distributions obtained from high energy antineutrino-nucleon charged-current interactions. We find that in general the behavior of the P_T^2 distributions and the invariant cross sections $F(x_F)$, $G(P_T^2)$ of the inclusive $K^o(\Lambda)$ data obtained from $\bar{\nu}N$ interactions are similar to those obtained from inclusive ep, νp and $\pi^- p$ data. The shape of the z-distribution for K^o mesons in the $z > 0.25$ region is described by the fragmentation model of Field and Feynman and does not contradict the νN data in this region. For Λ's the shape of the z-distribution is in good agreement with νN and electroproduced proton data.

We find that the average transverse momentum squared behavior for K^o mesons as a function of Q^2, W^2, x and z in the current fragmentation region is in qualitative agreement with the prediction of quantum chromodynamics (QCD). We find that $< P^2_{out} >$ for K^o's produced in $\bar{\nu}$ charged-current interactions rises with increasing Q^2 and W^2 but falls with increasing x.

Finally we have estimated polarization effects in $\bar{\nu}$ charged-current interactions. The longitudinal and transverse polarizations are compatible with zero, but a positive Λ polarization perpendicular to the production plane is observed at small x.

ACKNOWLEDGMENTS

We wish to thank the members of the Neutrino Laboratory at Fermilab and the scanning, measuring and secretarial staffs at our respective laboratories for their contribution to this experiment. This work was supported in part by the U.S. Department of Energy and the National Science Foundation.

REFERENCES

[1]L. M. Sehgal, Hadron Production by Leptons, Proc. of the Int. Symposium on Lepton and Photon Interactions, Hamburg, 1977 (DESY, 1977) 837.

[2]M. Derrick et al., Phys. Rev. D17 (1978) 17.

[3]J. P. Berge et al., Phys. Rev. D18 (1978) 1359.

[4]I. Cohen et al., Phys. Rev. Lett. 40 (1978) 1614.

[5]V. Luth et al., Phys. Lett. 70B (1977) 120.

[6]J. Burmester et al., Phys. Lett. 67B (1977) 367.

[7]J. P. Martin et al., Phys. Rev. Lett. 40 (1978) 283;
R. Brandelik et al., Phys. Lett. 67B (1977) 363.

[8]M. Aderholz et al., Hydra Application Library (1974).

[9]R. J. Cence et al., Nucl. Instr. Methods 138 (1976) 245.

[10]J. P. Berge et al., Study of Inclusive Neutral Currents with the Fermilab Broad-Band Antineutrino Beam in 15-ft Bubble Chamber, Proc. for the Int. Conference on Neutrino Physics, Baksan Valley, 1977 (Moscow, 1978) V2, 180.

[11]FIIM Neutrino Group, Phys. Rev. Lett. 39 (1977) 382.

[12]P. H. Stuntebeck et al., Phys. Rev. D9 (1974) 608.

[13]K. Hanson, Inclusive and Exclusive Virtual Photoproduction Results from Cornell, Proc. of the Int. Symposium on Lepton and Photon Interactions, Stanford, 1975 (SLAC, California 94305, 1975) 739.

[14]R. D. Field and R. P. Feynman, Nucl. Phys. B136 (1978) 1.

[15]R. B. Palmer, Lepton and Charm Production in the 15-ft Bubble Chamber, Proc. of the XIIIth Rencontre de Moriond, Les Arcs-Savoie, 1978 (28100 DREUX, France, 1978) v2, 361.

[16]L. Hand, Elastic and Inelastic Electron and Muon Scattering, Proc. of the Int. Symposium on Lepton and Photon Interactions, Hamburg, 1977 (DESY, 1977) 417.

[17]H. D. Politzer, Phys. Rep. 14C (1974).

[18]J. Bell et al., Phys. Rev. D19 (1979) 1.

[19]A. Mendez, Nucl. Phys. B145 (1978) 199.

[20]Particle Data Group, Rev. Mod. Phys. 48 (1976) 524.

[21]G. L. Kane and Y. P. Yao, Nucl. Phys. B137 (1978) 313.

TABLE I

NUMBER OF CHARGED-CURRENT EVENTS WITH ONE OR MORE K^o OR Λ.

CATEGORY [a]	OBSERVED EVENTS	CORRECTED EVENTS [b]
$\bar{\nu}N \to \mu^+ K^o X$	188 ± 14	355 ± 97
$\bar{\nu}N \to \mu^+ \Lambda X$	170 ± 13	253 ± 36
$\bar{\nu}N \to \mu^+ K^o \bar{K}^o X$	14 ± 4	199 ± 54
$\bar{\nu}N \to \mu^+ K^o \Lambda X$	17 ± 4	136 ± 32

a) X may contain in addition any number of charged strange particles. The corresponding number of observed charged-current events containing $\Lambda \to p\pi^-$ decays is three.

b) Corrected for potential length cuts, neutral decay modes (including K_L^o) and scanning and processing efficiencies.

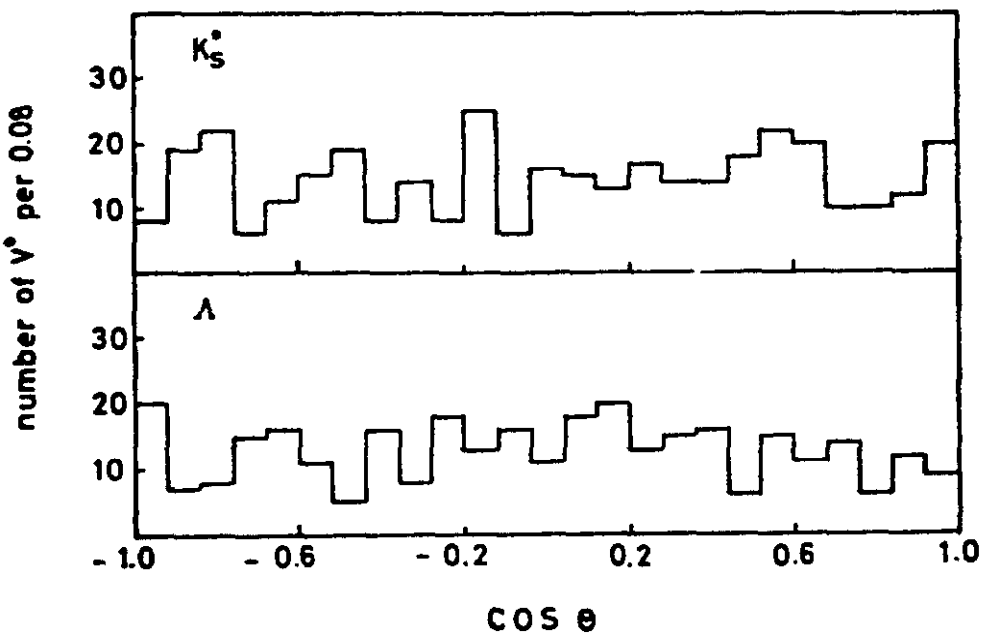

Fig. 1. Distribution of $\cos\theta$ for K_S^0 and Λ decays. Here θ is the decay angle of the π^+ (P) from the K_S^0 (Λ) decay with respect to the K_S^0 (Λ) direction in the lab, calculated in the K_S^0 (Λ) rest frame.

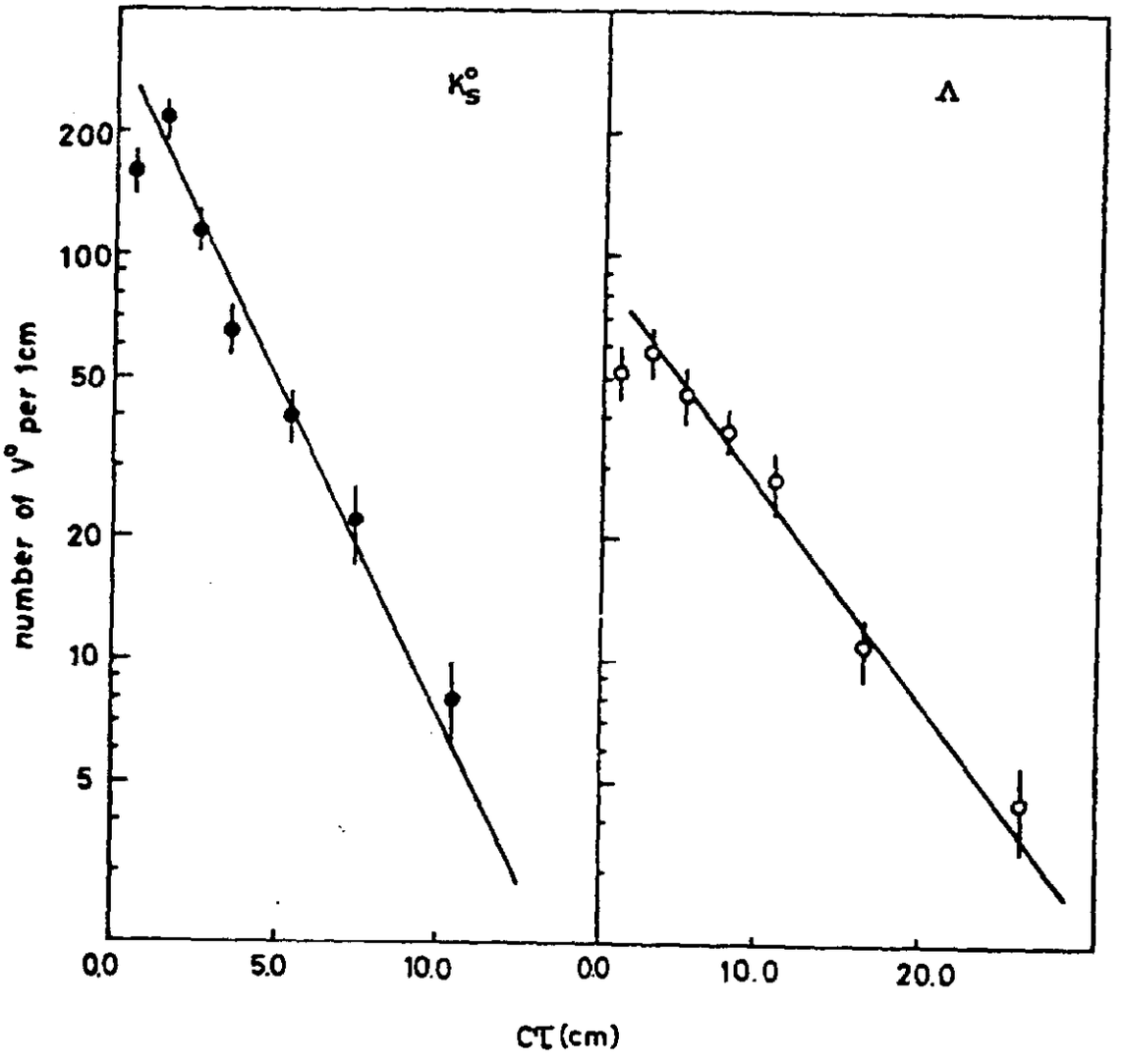

Fig. 2. Distribution of $c\tau$ (τ is the proper decay time) for the K_s^0 and Λ decay.

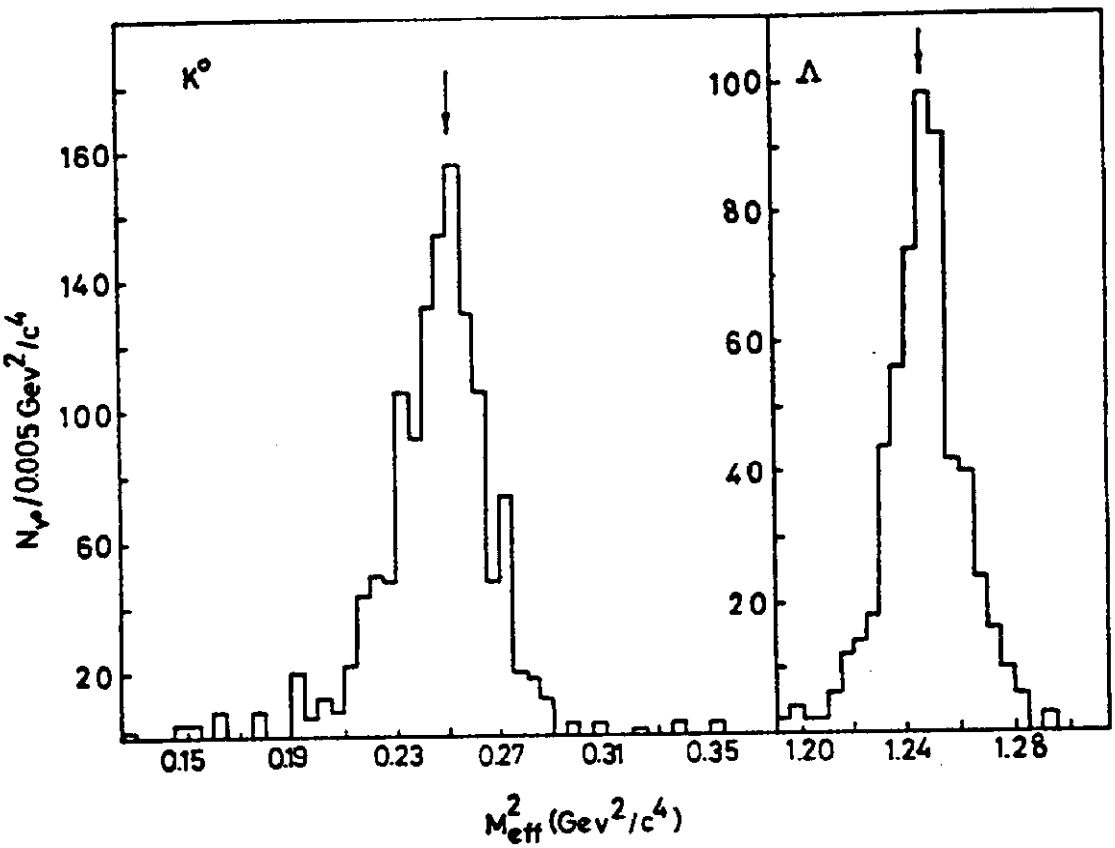

Fig. 3. The $\pi^+\pi^-$ ($p\pi^-$) effective mass squared distribution for K^0 (Λ).

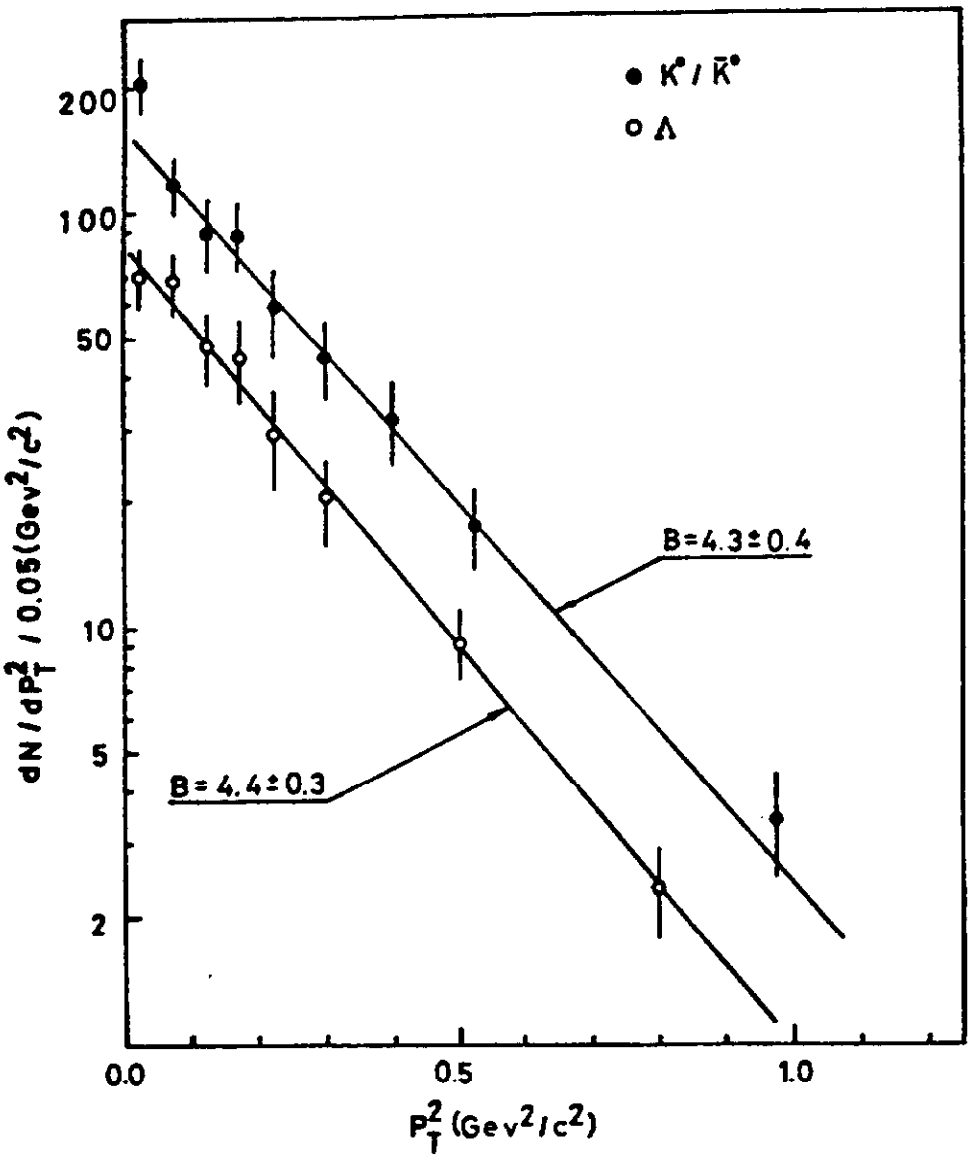

Fig. 4. The P_T^2 distributions for the K^0 and Λ. The lines show the results of fits to the exponential forms described in the text.

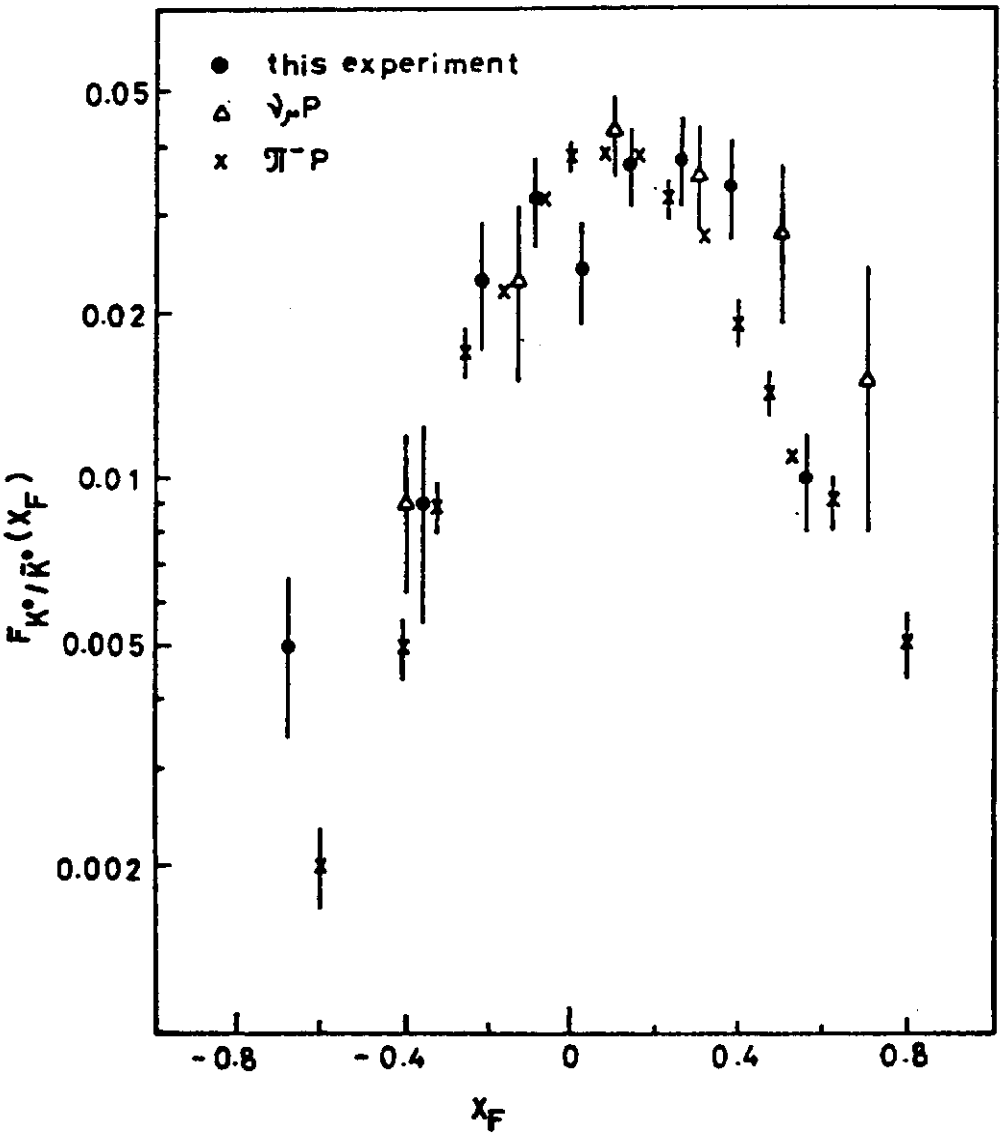

Fig. 5a. Invariant structure functions $F(x_F) = \int \phi(x_F, P_T^2) dP_T^2$ for K^0 mesons. The normalized νp, $\pi^- p$ and ep data are shown.

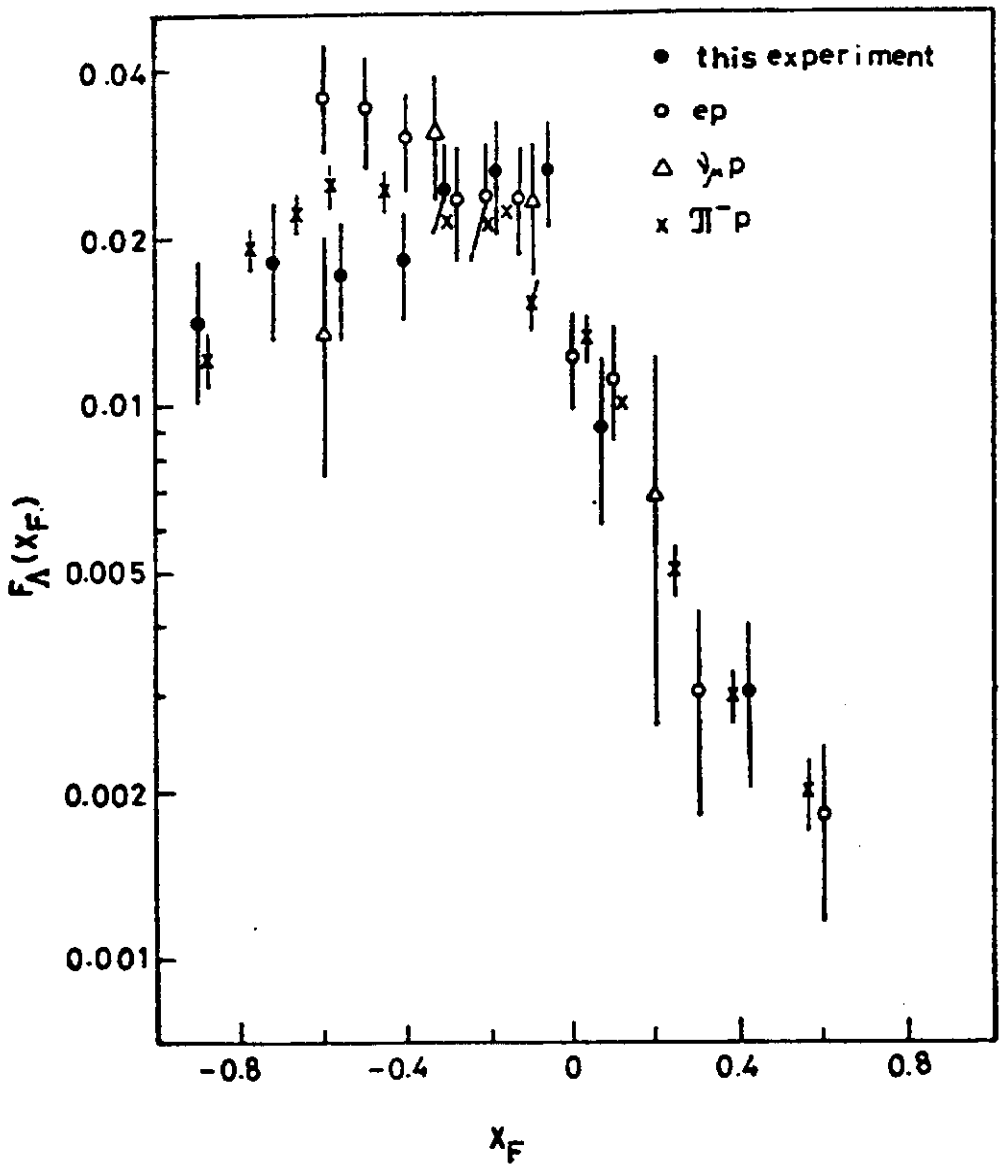

Fig. 5b. Invariant structure functions $F(x_F) = \int \phi(x_F, P_T^2)\, dP_T^2$ for Λ hyperons. The normalized νp, $\pi^- p$ and ep data are shown.

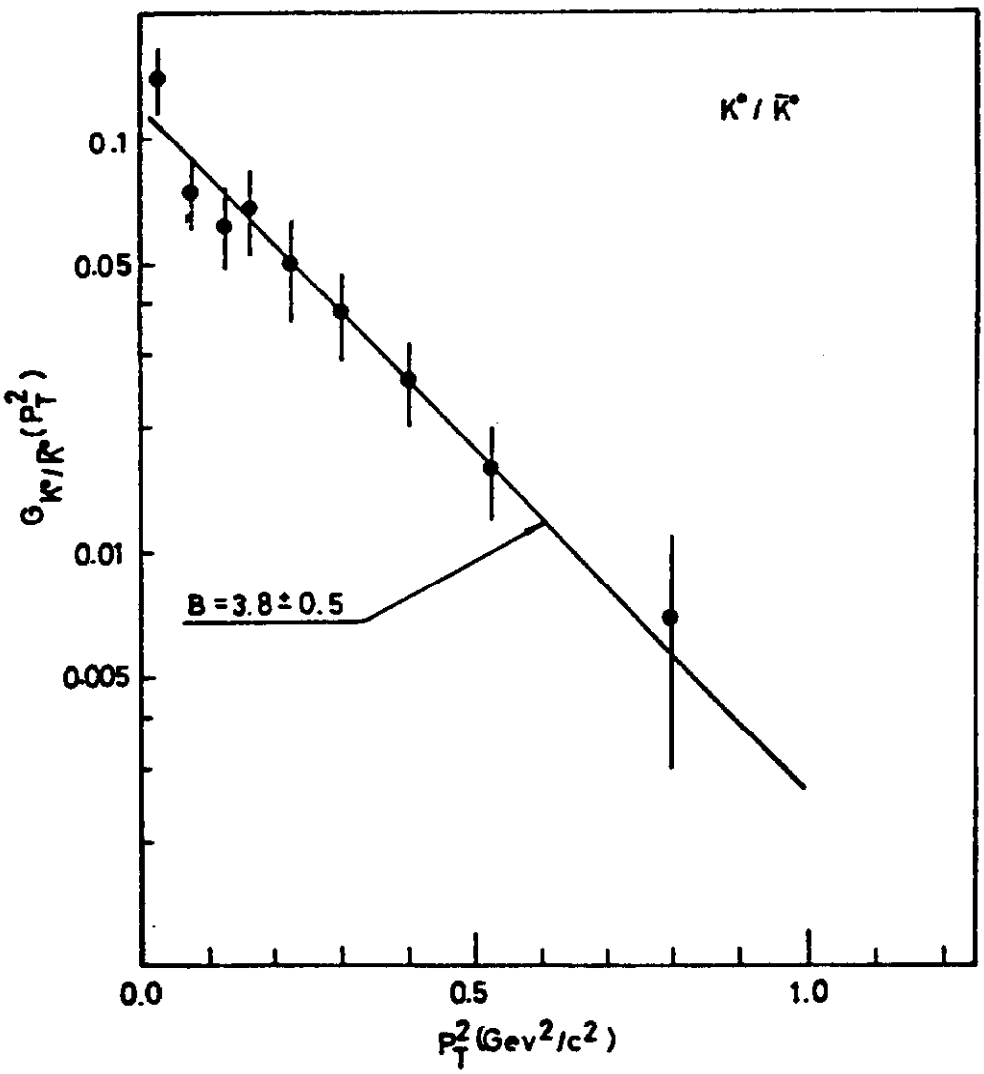

Fig. 6a. Invariant cross sections $G(P_T^2) = \int \phi(x_F, P_T^2)\, dx_F$ for K^0. The solid lines represent results of fits to the form $a \cdot \exp(-bP_T^2)$.

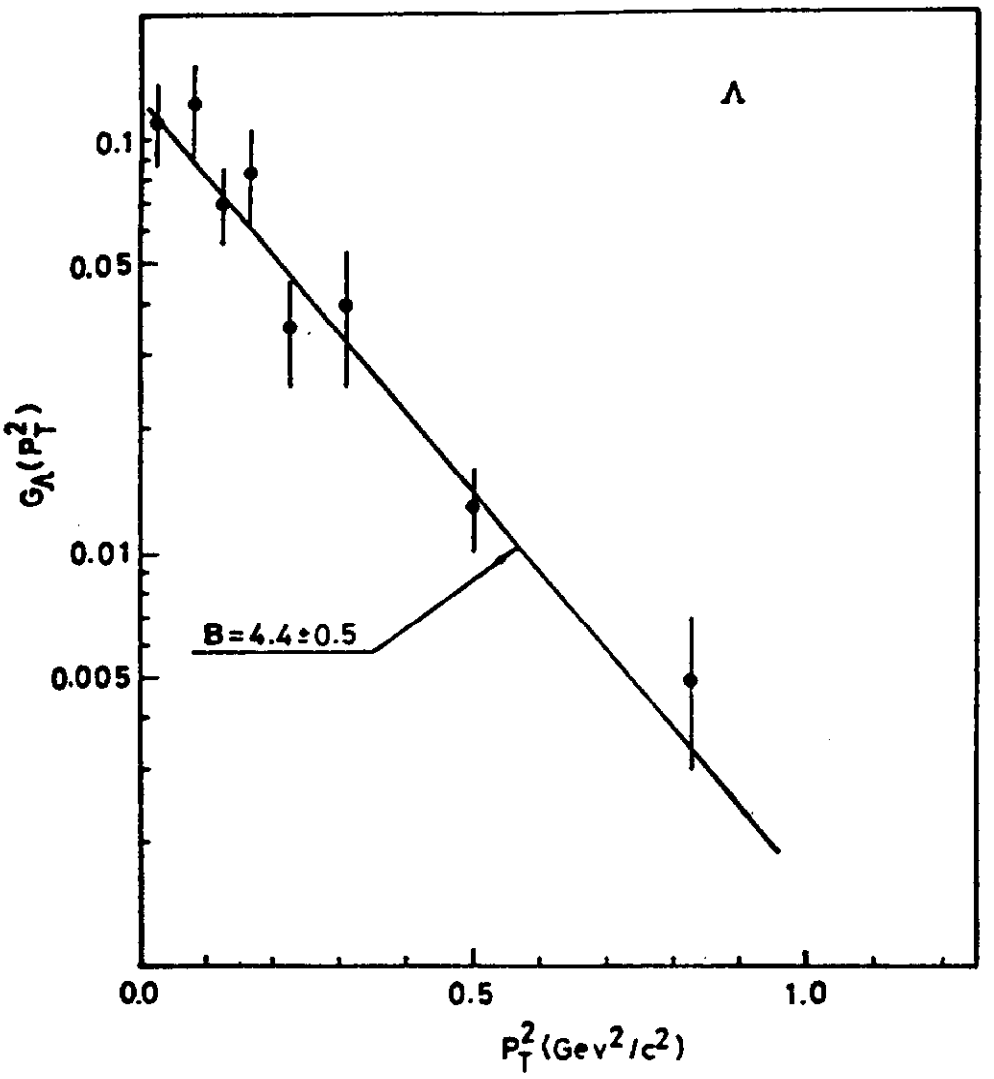

Fig. 6b. Invariant cross sections $G(P_T{}^2) = \int \phi(x_F, P_T{}^2)\, dx_F$ for Λ. The solid lines represent results of fits for the form $a \cdot \exp(-bP_T{}^2)$.

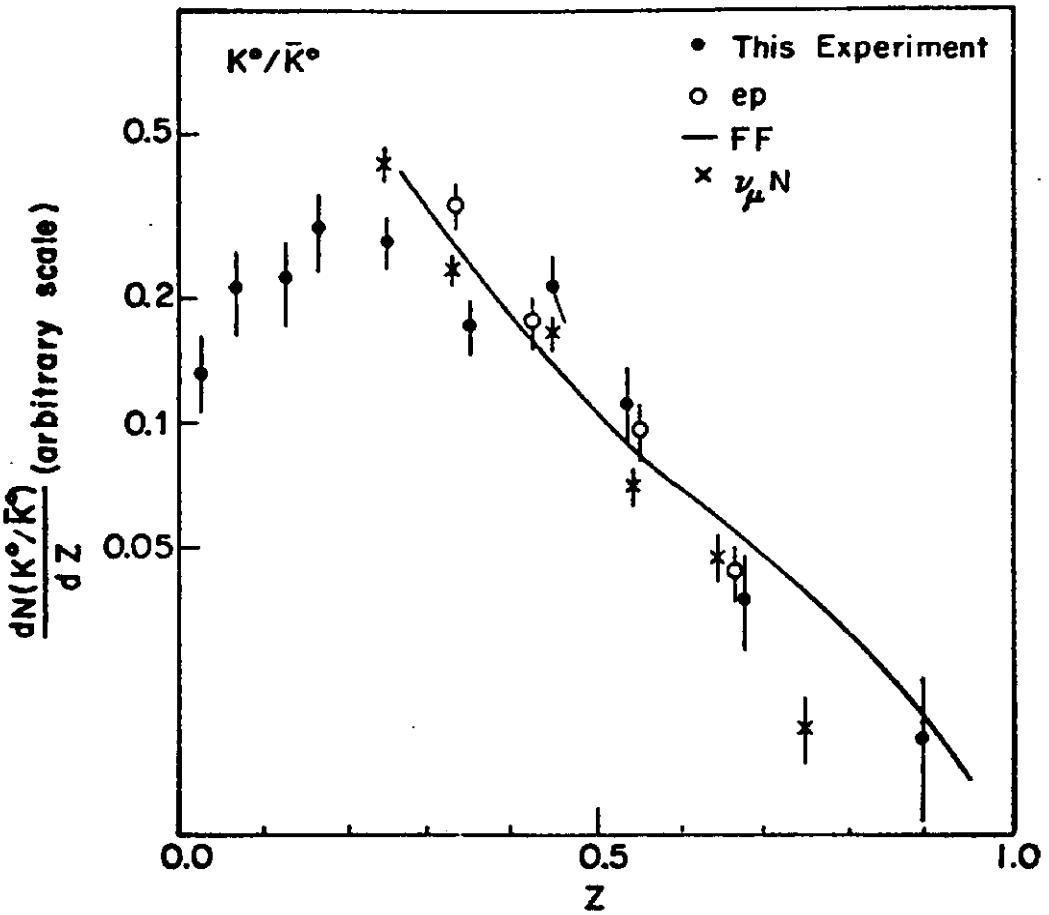

Fig. 7a. Z distribution for K^0 mesons compared with those from ep and νN experiments. The curve shows the results of the fragmentation function calculation of FF2.

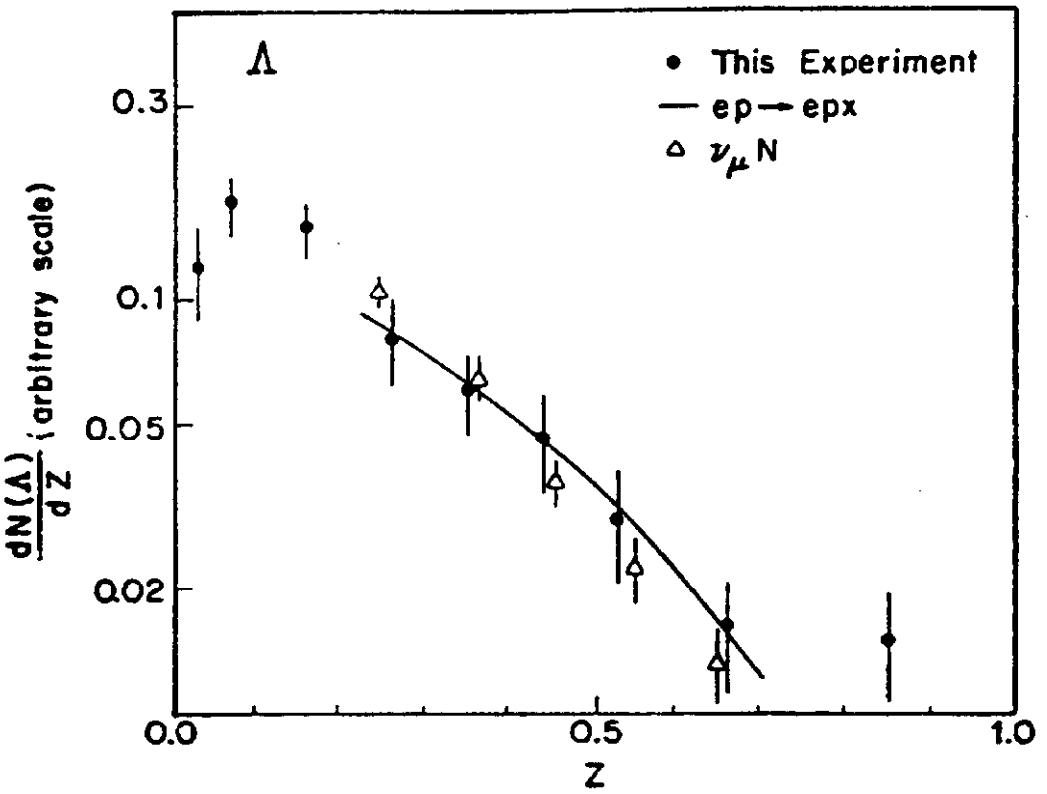

Fig. 7b. Z distribution for Λ^1s together with νN data. The solid line represents the shape of electroproduced protons.

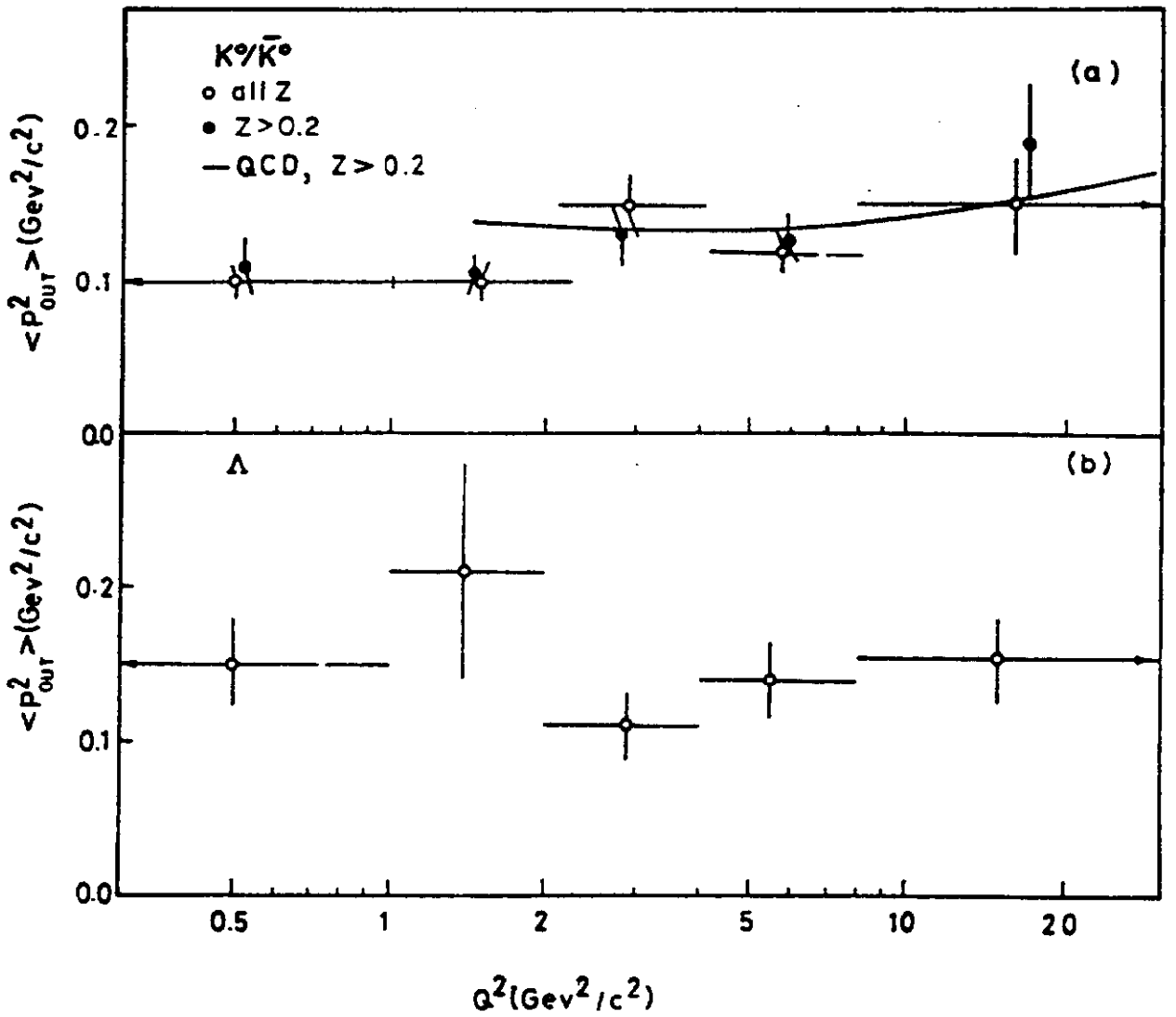

Fig. 8. Distribution of $< P^2_{out} >$ for K^0 (a) and Λ (b) with respect to Q^2. The solid curve represents the QCD calculation described in the text for K^0's with $z > 0.2$.

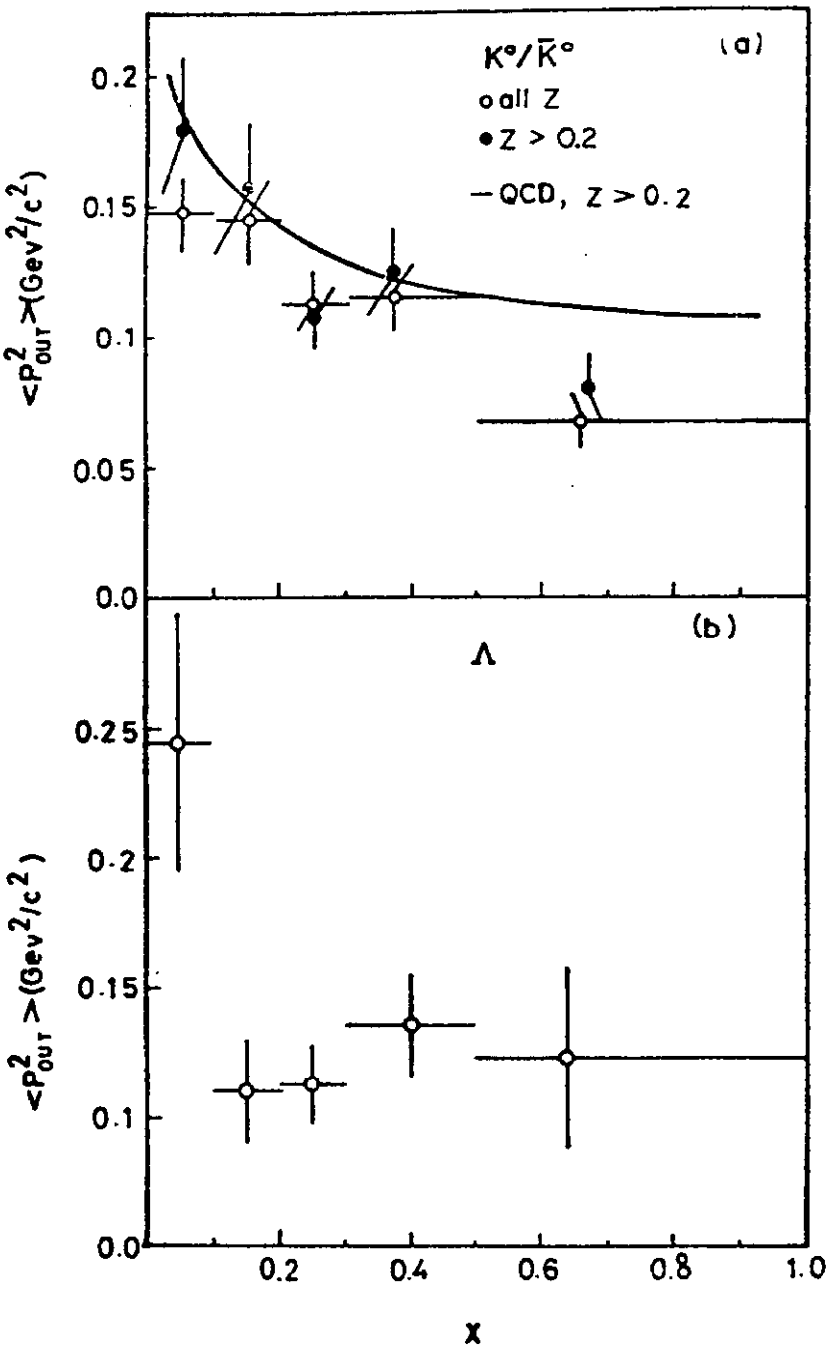

Fig. 9. Dependence of $< P^2_{out} >$ versus x for K^0 (a) and Λ (b). For K^0 mesons the QCD predictions are shown by the solid curve in the region z > 0.2.

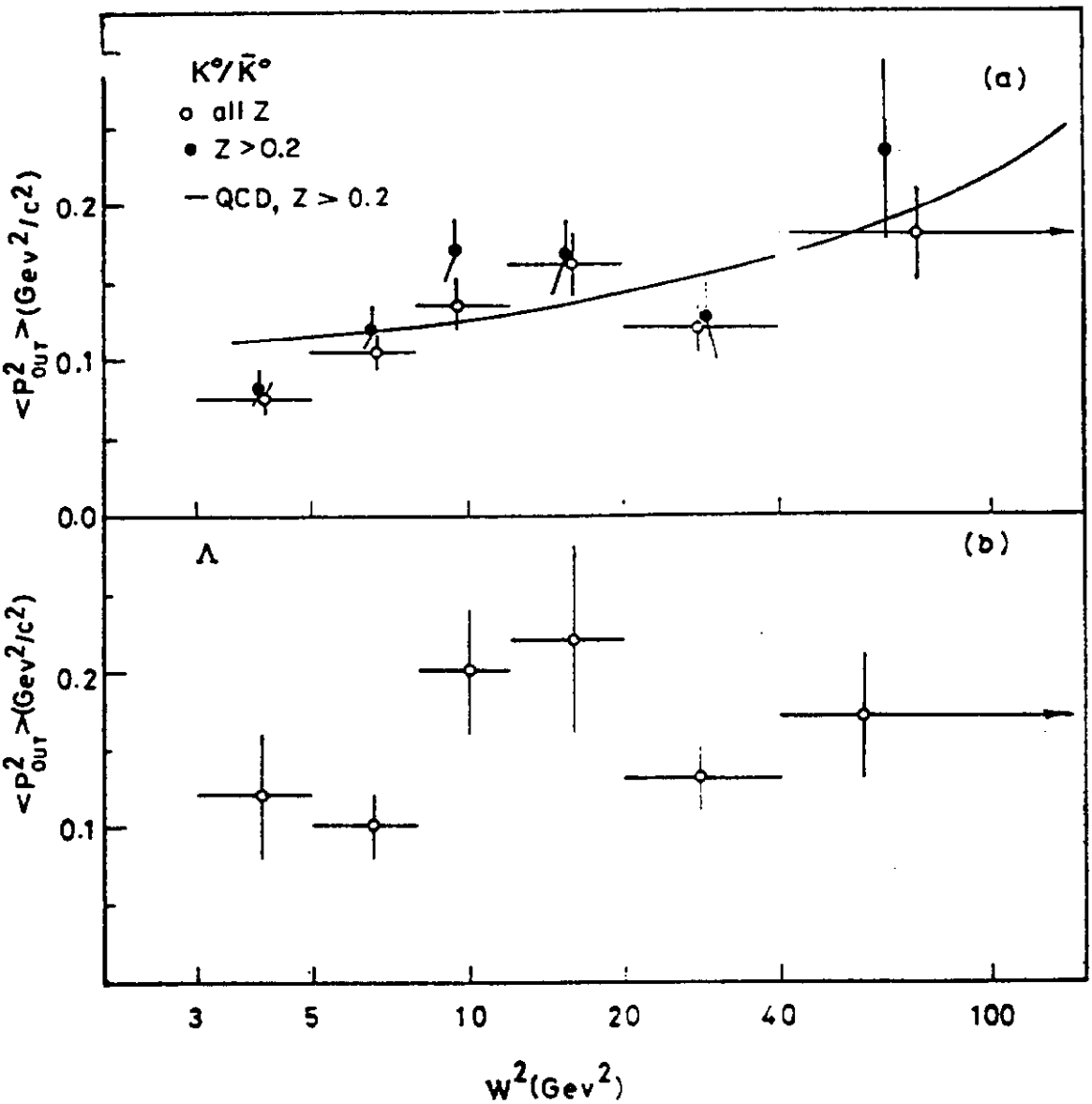

Fig. 10. Distribution of $< P^2_{out} >$ for K^0 (a) and Λ(b) as a function of W^2. The curve gives the QCD prediction for the K^0 mesons in the current fragmentation region.

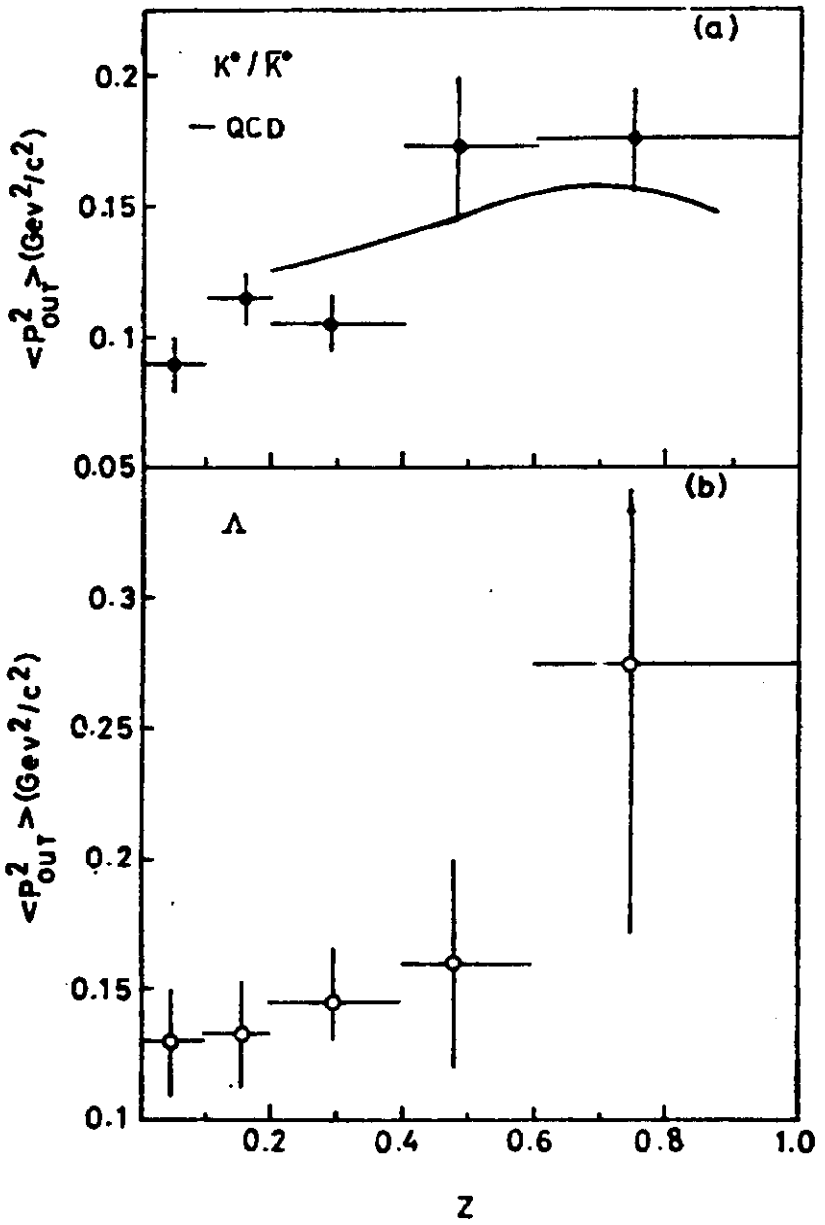

Fig. 11. Dependence of $< P^2_{out} >$ versus z for K^0 mesons (a) and Λ's (b). QCD predictions for K^0's are shown by the solid curve.

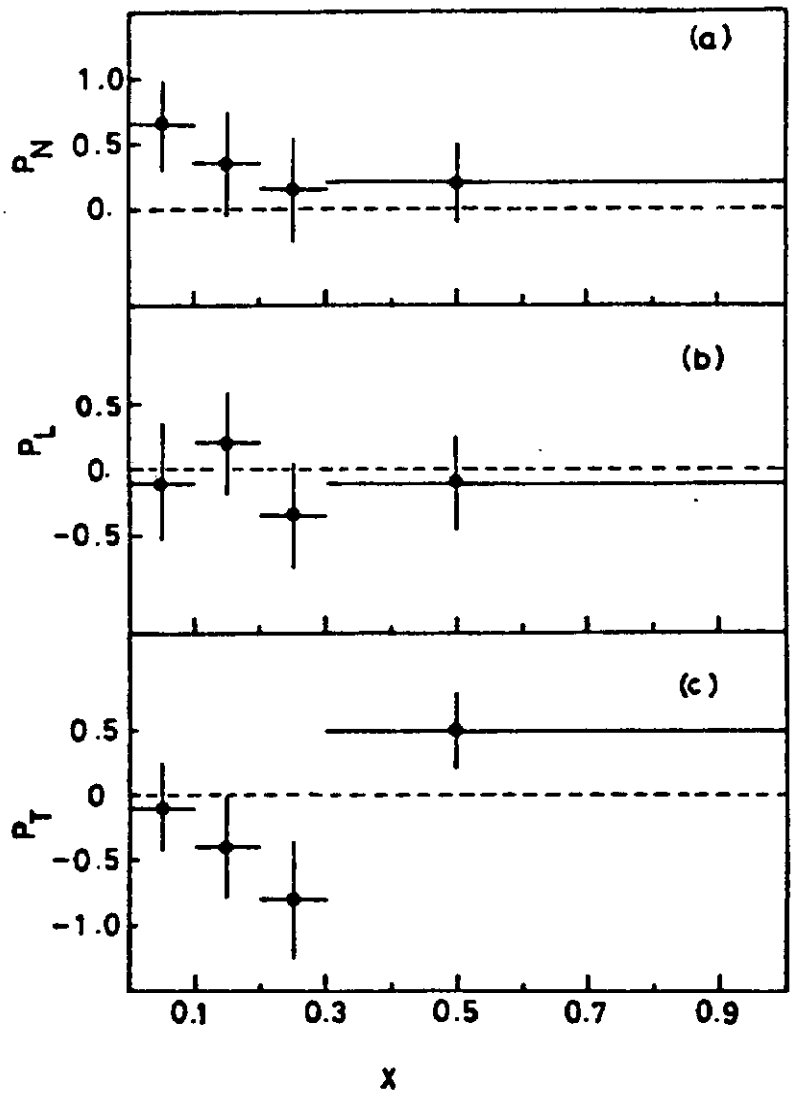

Fig. 12. Normal (a), longitudinal (b) and perpendicular (c) polarization of Λ hyperon as a function of $x = Q^2/2m\nu$.

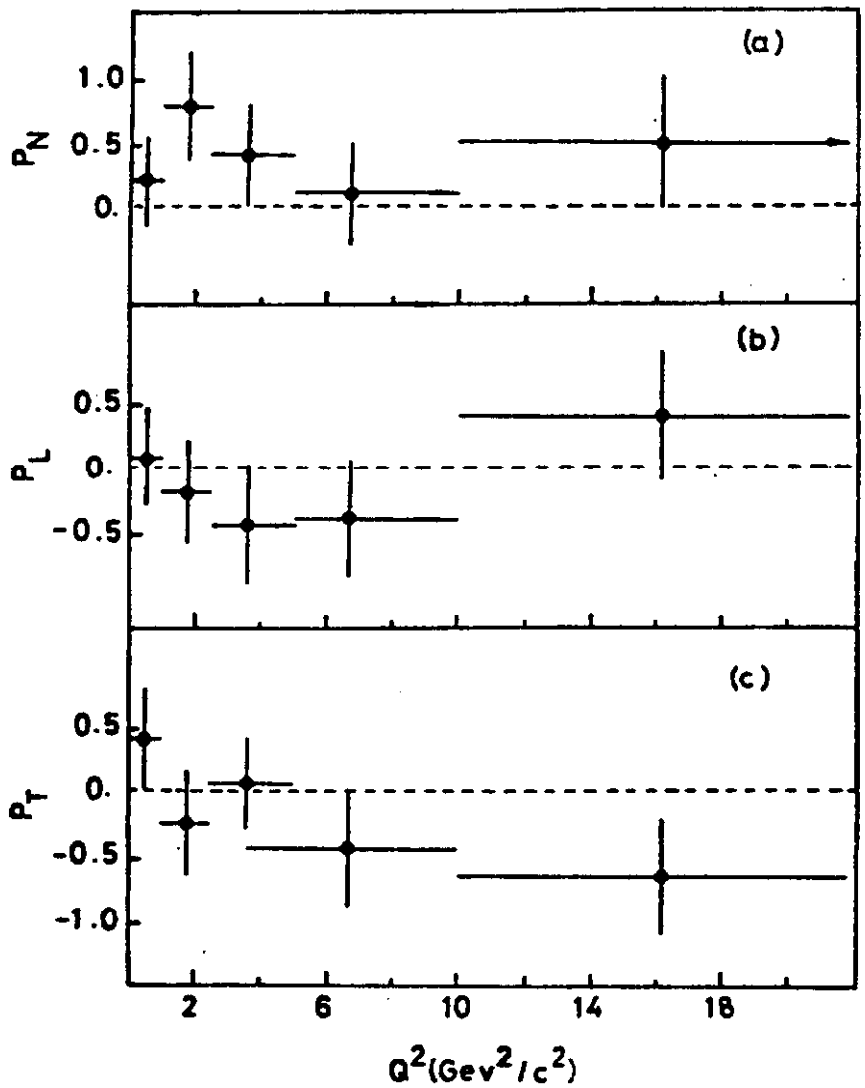

Fig. 13. Normal (a), longitudinal (b) and perpendicular (c) polarization of Λ hyperon as a function of Q^2.